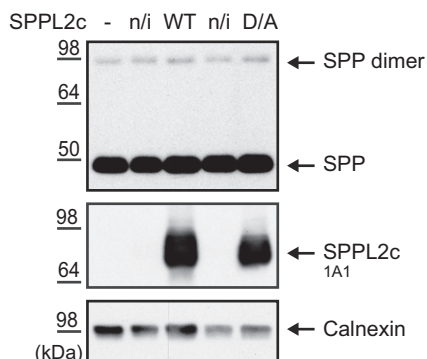
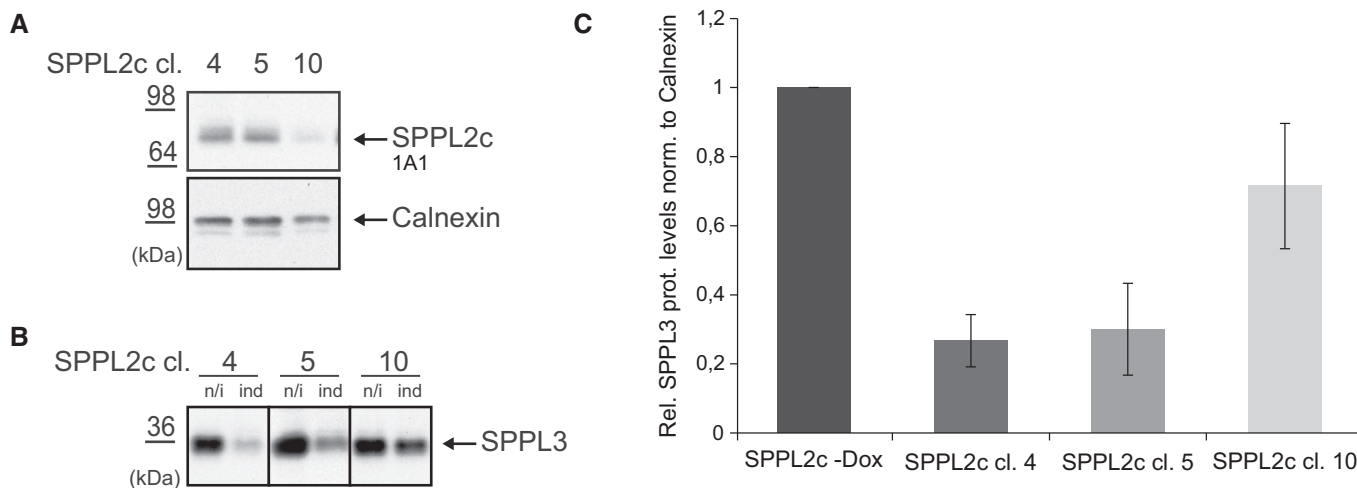


Expanded View Figures

**Figure EV1. SPP expression is not affected by SPPL2c overexpression.**

Western blot analysis depicting the SPP expression levels in control HEK293 cells (-), cells overexpressing wild-type SPPL2c (WT, ind) or catalytically inactive SPPL2c (D/A, ind) and their non-induced (n/i) controls. Calnexin served as loading control, and ectopic expression of SPPL2c WT and SPPL2c D/A was confirmed using the monoclonal SPPL2c-specific antibody. Note that neither SPP monomer nor SPP dimer is changed in SPPL2c-expressing cells compared to control cells. Source data are available online for this figure.

**Figure EV2. SPPL3 expression decreases upon SPPL2c overexpression.**

A Western blot analysis depicting the ectopic SPPL2c expression of three independent HEK293 cell clones. Calnexin served as loading control.

B Western blot analysis depicting the SPPL3 expression levels in the three SPPL2c clones under non-induced (n/i) and induced (ind) conditions.

C Quantification of endogenous SPPL3 protein levels from Fig EV2B normalized to Calnexin ($n = 4$). Depicted are the ratios of SPPL3 expression before and after induction of SPPL2c overexpression with doxycycline for each SPPL2c-expressing clone shown in (A). SPPL3 expression of all three non-induced clones is set to 1 (SPPL2c-Dox). Mean \pm SD. Note that clone number 10 depicts the highest SPPL3 expression and the lowest exogenous SPPL2c expression.

Source data are available online for this figure.

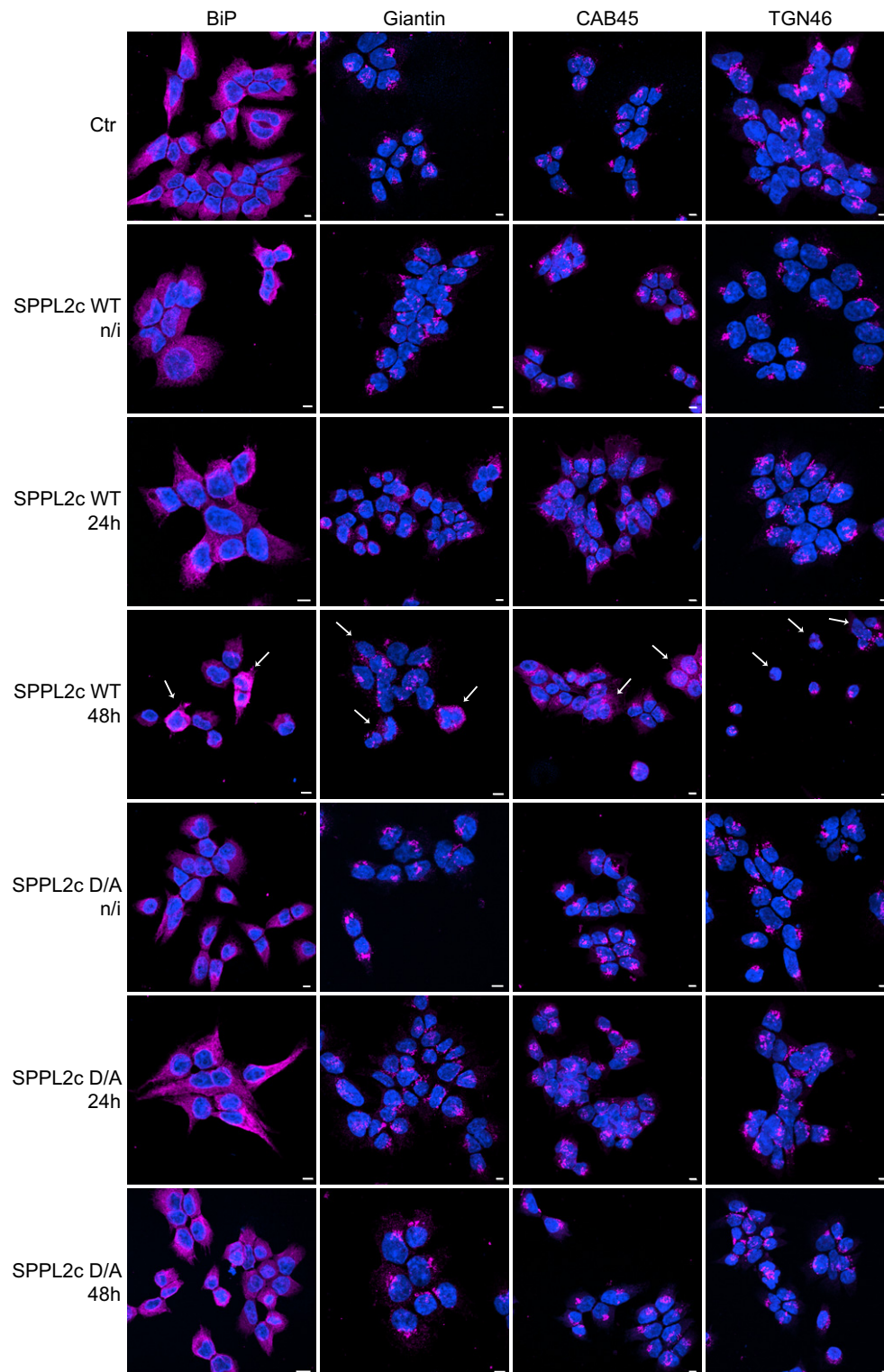


Figure EV3. ER and Golgi morphology in HEK293 cells with ectopic expression of SPPL2c.

Cells were seeded and cultured for 72 h and expression of catalytically active (WT) or non-active (D/A) SPPL2c was induced by addition of doxycycline for either 24 or 48 h as indicated. Non-transfected cells (Ctr) or non-induced SPPL2c cells (n/i) served as controls. The ER was stained with the anti-BiP antibody, the *cis*/medial-Golgi with the anti-Giantin, the *trans*-Golgi network with the anti-TGN46 antibody, and all Golgi subcompartments with the CAB45-specific antibody. Note that only upon expression of catalytically active SPPL2c, the morphologies of ER and *cis*-Golgi change compared to controls. The most representative changes are indicated with white arrows at SPPL2c WT 48 h. This figure contains a smaller magnification of the same experimental setup as in Fig 5D. Scale bar 5 μ m.

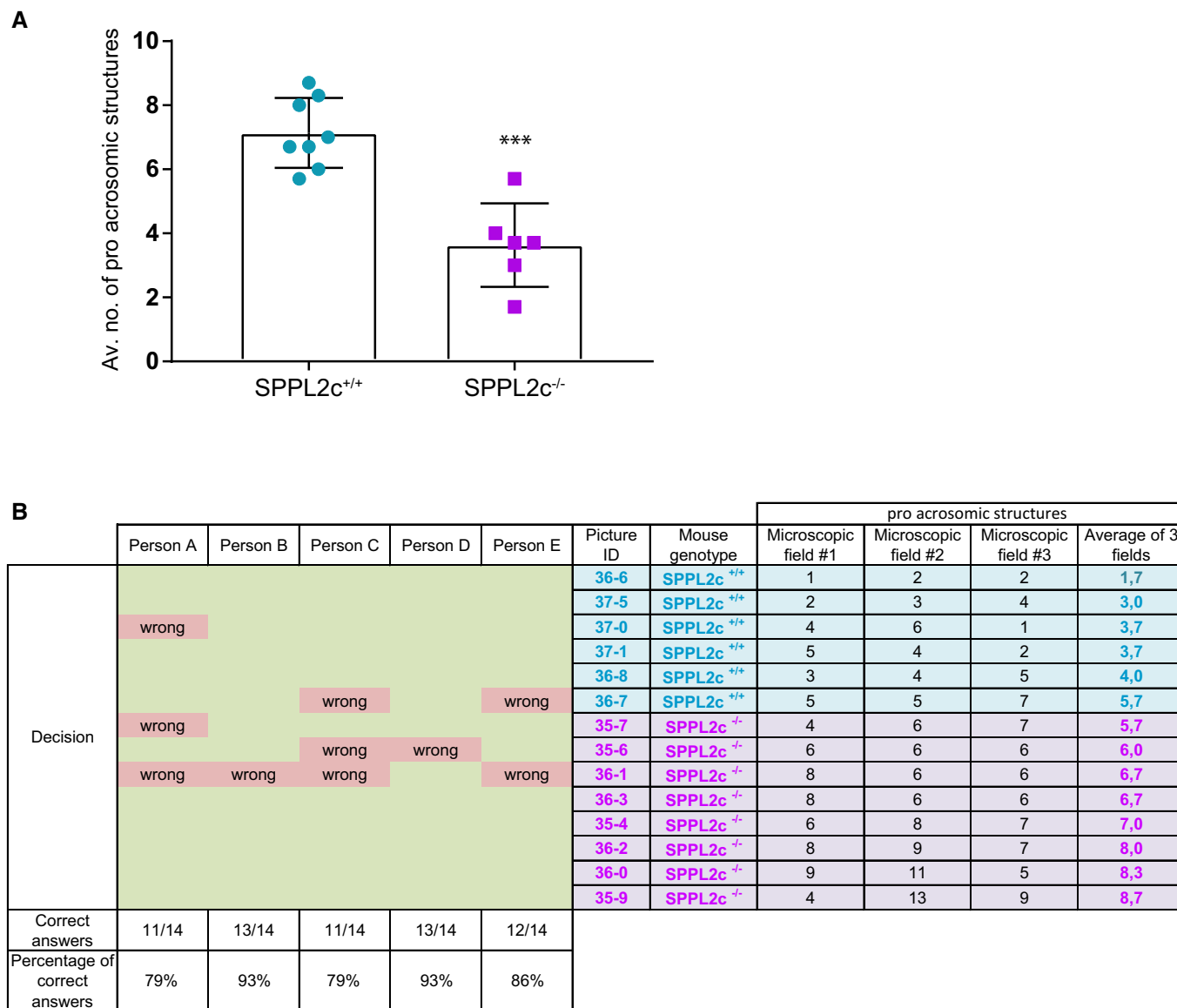


Figure EV4. Quantification of pre-acrosomal structures in seminiferous tubular cross sections.

A Pre-acrosomal resembling structures stained immunohistochemically with Cab45 (Fig 6F, black arrows) were quantified in $n = 14$ stage VII/VIII seminiferous tubules ($n = 6$ SPPL2c^{+/+} (petrol) and $n = 8$ SPPL2c^{-/-} (lilac) as described in Materials & Methods. The average number of stainings per tubule is depicted for each genotype, mean \pm SD. Unpaired, two-sided Welch's t -test. *** $P < 0.001$ ($P = 0.0004$).

B Table depicting the stainings counted for each single picture (microscopic fields #1–3) as well as the “average of 3 fields” plotted on Fig EV4A. The genotype of each mouse is indicated, as well as the blinded assignment of the pictures by five independent people, accompanied by the number and percentage of correct evaluations.

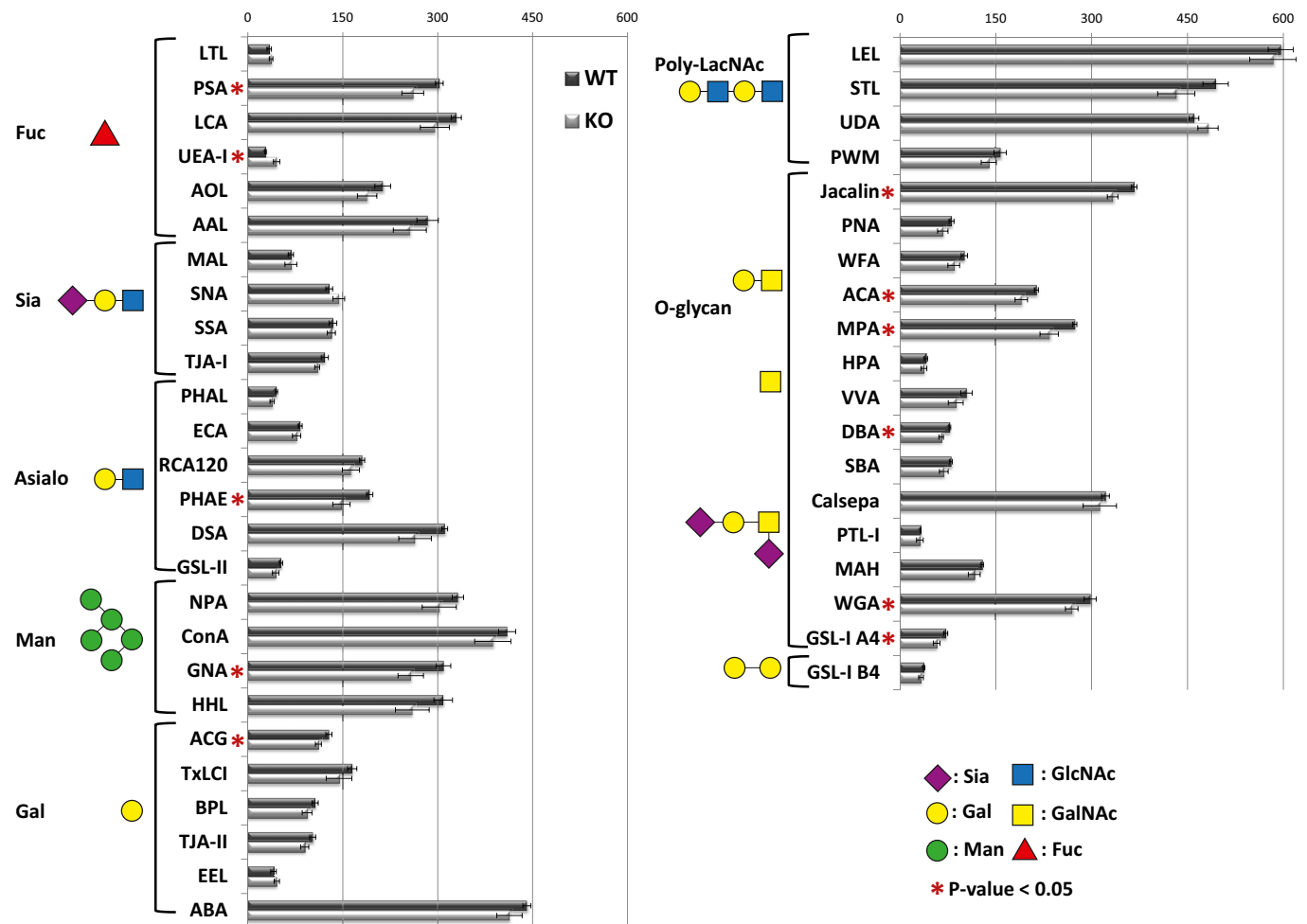


Figure EV5. Glycome fingerprint of mature spermatozoa isolated from the cauda epididymis of SPPL2c^{-/-} and control mice. The lectins that were significantly changed are marked with a red asterisk (*P*-value < 0.05, unpaired, two-sided Student's *t*-test, *n* = 4 animals per genotype).